Extended Abstracts of the 2020 International Conference on Solid State Devices and Materials, VIRTUAL conference, 2020, pp303-304

Void Engineering in Epitaxially Regrown Photonic Crystal Surface Emitting Lasers

Adam F. McKenzie[1,2], Ben C. King[1], Katherine J. Rae[1], Neil D. Gerrard[1], Jonathan R. Orchard[2], Kenichi Nishi[3], Keizo Takemasa[3], Mitsuru Sugawara[3], Richard J. E. Taylor[1], David T. D. Childs, Donald A. MacLaren[1], and Richard A. Hogg[1]

[1] University of Glasgow
University Avenue, Glasgw Q12 8QQ, UK
E-mail: a.mckenzie.1@research.gla.ac.uk
[2] CST Global Ltd.
4 Stanley Boulevard, Blantyre G72 0BN, UK
Phone: +44 1698 722072
[3] QD Laser Inc.
1-1 Minamiwatarida-cho, Kawasaki-ku, Kanagawa 210-0855, Japan

Abstract

The engineering of void structures in GaAs-based photonic crystal surface emitting lasers realised by epitaxial regrowth is demonstrated. AlAs growth on patterned GaAs is employed to enhance void formation due to its low mobility. Scanning transmission electron microscopy of AlAs/GaAs superlattices allows a snapshot of the growth front to be made, revealing the dominant growth planes and their relative growth rates. Choice of a suitable starting grating structure allows the radius, height, and asymmetry of the void to be engineered to enhance output power.

1. Introduction

Photonic crystal surface emitting lasers (PCSELs) are an emerging class of semiconductor laser. The inclusion of a photonic crystal (PC) grating layer adjacent to the active region enables single-mode vertical emission through the band-edge resonance effect, which promises area-scalable output powers without degradation of optical mode quality [1].

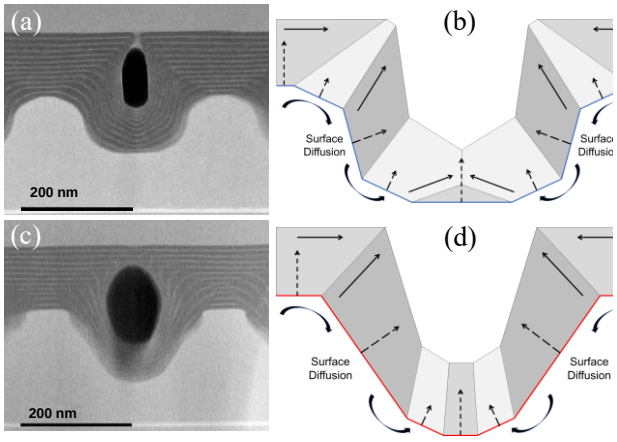

Figure 1. TEM images (a and c) and schematics (b and d) illustrating the evolving growth fronts and void formation during regrowth of devices A and B, respectively.

Whilst traditionally fabricated by wafer bonding, MOVPE-based epitaxial regrowth of the PC has proven advantageous in realising both all-semiconductor [2,3] and void-based PCSELs [4], with watt-class operation having been achieved in the latter case [4]. As properties such as coupling strength and output power are dependent on the grating geometry (thickness, r/a, n_{eff}) of the PC layer, control over the size and shape of the embedded voids is vital for optimising device characteristics.

In this paper, we present GaAs-based PCSELs containing voids embedded by epitaxial regrowth of the etched GaAs with an AlAs/GaAs superlattice. The effects of PC grating geometries on void formation are studied by transmission electron microscopy (STEM) analysis, and correlated to LI and spectral characteristics of the devices. The mechanism of void formation is highlighted through the inclusion of GaAs guide layers in the regrown AlAs layer, revealing a route to further device optimisation by tailoring of growth conditions.

2. Device Fabrication

Base-epitaxial structures including three GaInAs/GaAs quantum wells (tuned to emit at 1064 nm) and a top p-type GaAs layer were grown on 2 °-offcut (100) GaAs substrates by molecular beam epitaxy. A square-lattice PC with a period of 320 nm was defined in the top GaAs layer by reactive ion etching. The patterned wafer was then loaded into a Thomas Swan 3x2″ CCS MOVPE reactor and regrown with an AlAs/GaAs (9nm/1nm) superlattice structure at 650 °C, followed by p-AlGaAs cladding and p+-GaAs contact layers. The PC grating profiles of the devices were varied via mass-transport during the pre-growth temperature ramp within the reactor prior to regrowth. Fabrication was completed by the deposition of electrical contacts and bond pads, and the opening of a 60 µm-diameter emission window on the surface of the device [2].

3. Regrowth and Device Analysis

Cross-sectional STEM images of two devices reveal the effect of pre-growth mass-transport on the profile of the PC

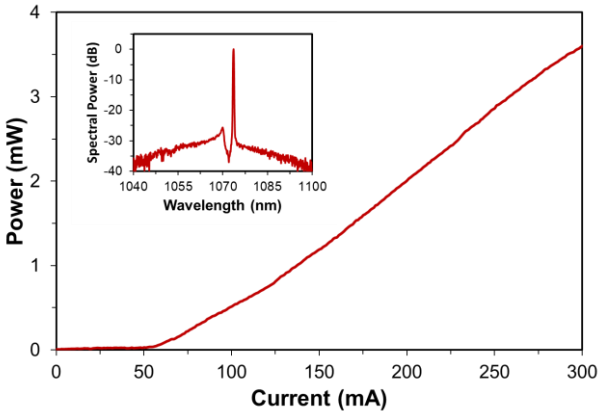

Figure 2. Pulsed LI characteristics and lasing spectrum (inset) of device B showing threshold current of 65 mA and emission at 1074 nm.

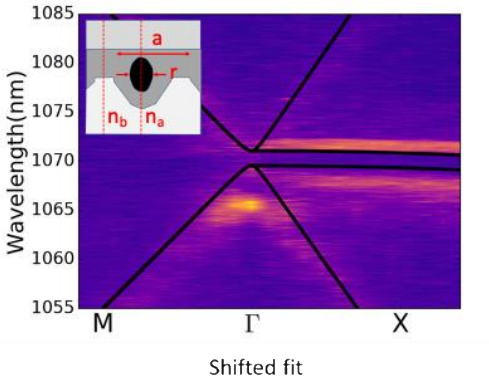

Figure 3. Measured and simulated (overlay) band structure of device B. Model used for simulation (inset) constructed from TEM image.

grating. In device A (figure 1a), diffusion under an AsH_3 overpressure results in significant broadening of the grating profile along with a reduction in depth; in addition, (311)-type planes have formed at the top and bottom of each grating hole. A reduction in ramp time (figure 1c) resulted in minimal deformation, with the retention of the depth and (111)-type sidewalls of the original grating etch. The evolution of the growth front during regrowth for each device is illustrated in figure 1b and d.

In both cases crystallographic voids form within the PC layer, each with a unique geometry that is a consequence of the grating profile at the start of deposition. Overall, formation is driven by lateral growth of the top (100) plane towards the center of the grating hole where circumferential growth fronts coalesce to embed the void. The rate of lateral growth is dependent on the plane adjacent to the top (100) and competes with growth from planes within the grating hole to determine the size and shape of the void. In the case of device A, the presence of (311) planes results in the formation of a "pill"-shaped void with vertical sidewalls, whereas the reduced growth rate on the (111) sidewalls in device B leads to a significantly larger "egg"-shaped void, as seen in figure 1.

Of the two devices, B displayed superior performance under pulsed conditions (2 µs pulse width, 1 % duty cycle, 20 °C) (figure 2), with a reduced threshold current of 65 mA (vs 440 mA for A), and a slope efficiency of 0.015 W/A. The low slope efficiency is in part due to the loss of light emitted into the substrate, coverage of the emission area by the gold contact, and comparatively small dimensions resulting in significant in-plane losses.

The improvements in performance can be attributed to the larger void volume in this device. The larger r/a associated with the PC provides more favourable values of the in- and out-of-plane coupling coefficients leading to reduced threshold current [5], whilst the increased void height and vertical asymmetry result in greater output power by the suppression of destructive interference [6,7]. Figure 3 shows band structure simulation of device B, performed on a model constructed using the TEM image as a basis, showing good correlation between measured and simulated devices.

4. Conclusions

STEM imaging has been used to reveal the mechanism for void formation in regrown PCSELs utilising an AlAs/GaAs superlattice. This technique provides a series of snapshots of the growth front, and highlights routes to future device optimisation by engineering of growth parameters and/or grating profile.

References

[1] K. Ishizaki *et al.*, Photonics **6** (2019) 96
[2] D. M. Williams *et al.*, IEEE Photon. Technol. Lett. **24** (2014) 966
[3] R. J. E. Taylor *et al.*, Sci. Rep. **5** (2015) 13203
[4] K. Hirose *et al.*, Nature. Photon. **8** (2014) 406
[5] R. J. E. Taylor *et al.*, IEEE J. Select. Topics Quant. Electron. **19** (2013) 4900407
[6] S. Iwahashi *et al.*, J. Opt. Soc. Am. B **27** (2010) 1204
[7] C. Peng *et al.*, Opt. Express **19** (2011) 24672